arXiv:1603.05420v1 [nlin.PS] 17 Mar 2016

On the interaction of uni-directional and bi-directional buckling of a plate supported by an elastic foundation

M. Khurram Wadee[1], David J.B. Lloyd[2], and Andrew P. Bassom[3]

[1]College of Engineering, Mathematics and Physical Sciences, University of Exeter, Exeter, EX4 8EL, UK
[2]Department of Mathematics, University of Surrey, Guildford, GU2 7XH, UK
[3]School of Mathematics and Physics, University of Tasmania, Private Bag 37, Hobart 7001, Australia.

March 18, 2016

Abstract

A thin flat rectangular plate supported on its edges and subjected to in-plane loading exhibits stable post-buckling behaviour. However, the introduction of a nonlinear (softening) elastic foundation may cause the response to become unstable. Here the post-buckling of such a structure is investigated and several important phenomena are identified, including the transition of patterns from stripes to spots and back again. The interaction between these forms is of importance for understanding the possible post-buckling behaviours of this structural system. In addition, both periodic and some localized responses are found to exist as the dimensions of the plate are increased and this becomes relevant when the characteristic wavelengths of the buckle pattern are small compared to the size of the plate. Potential application of the model range from macroscopic industrial manufacturing of structural elements to the understanding of micro- and nano-scale deformations in materials.

1 Introduction

Instability in elastic bodies is of practical importance to engineers who are responsible for the design of safe structures. If our sole concern was to understand the initial stages of buckling of such bodies then a suitable model consisting of linearized equations would serve the purpose. On the other hand a deeper appreciation of the true nature of the buckling together with knowledge of the properties of later stages of the failure mechanisms requires that nonlinear effects be included as well. In the overwhelming majority of post-buckling scenarios exact analytical solutions do not exist and so, necessarily, we have to resort to approximation, be it fully numerical or a simplification of the full system followed by analysis in various limited regimes [28]. Both of these strategies can reveal behaviour which is of interest not only to engineers but to applied scientists and mathematicians as well. Instability phenomena are becoming of increasing importance in many fields [6] and some previous studies are being given renewed prominence owing to the discovery of physical phenomena down to the atomic level which these theories seem to model well [22]. It is in this spirit that here we study a problem that at first sight seems to be a simplistic two-dimensional extension of an exhaustively-studied one, namely the buckling of a strut resting on an elastic foundation.

In structural engineering, plates are used as load-bearing elements in various guises, including floor slabs, retaining walls, pad foundations, ship hulls and aircraft wings. Of these, perhaps the pad would most naturally be modelled by a plate on a foundation. There are examples where certain parts of structural components can be modelled as plates which are supported; an obvious candidate is a sandwich panel for which a core supports a pair of thin skins. Several of these problems have been examined assuming

one-dimensional behaviour and our intention is to extend these ideas to incorporate a second dimension. Moreover the importance of supported plates is not limited to large-scale structures for similar systems have been proposed as models to look at thin elastic films supported by a substrate. There has been much work on one-dimensional *wrinkling* (another form of buckling) either when a specimen is compressed or if the supporting substrate (foundation) is pre-stretched when the elastic layer is placed on it and is then released. The plate equations for such a configuration have been solved using a finite-element technique and compared with experimental data [3]. Moreover, rather than just being an unfortunate by-product of loading, wrinkling in some physical systems may actually be desirable and its control can be effected by judicious application of load in various directions [38].

At an even smaller scale, studies have shown that wrinkling of nano-scale materials can be sufficient to modify electrical, optical and other physical properties. In particular compressed graphene behaves in this way and a useful model for this material is that of an isolated elastic layer [35]. We believe that improved understanding of wrinkling in nano-materials might be gained by incorporating a supporting elastic medium as an integral part of the system.

The well-studied one-dimensional strut model has numerous applications from the buckling of submarine pipelines and railway tracks through to sandwich panels and as a phenomenological model for various shell structures [7, 24, 27]. Various mathematical techniques have been utilized to study this system including Rayleigh–Ritz and Galerkin analyses [34], multiple-scale perturbation expansions [16, 20] and advanced hyperasymptotic methods [8, 32]. Part of the motivation for this flurry of activity has been the fact that the strut model can be regarded as a member of a family of problems governed by a Swift–Hohenberg (SH) equation. The SH equation is a partial differential equation in both time and space that simplifies to an ordinary differential equation (ODE) form when interest is restricted to time-invariant behaviour in one spatial dimension. Static equilibria and their stability can readily be deduced from this reduced problem. A key distinction between the strut and plate models is that the former is of unbounded length—suitable for the study of very long structures—and solutions sought can be periodic or homoclinic (localized in extent) where deflection approaches zero in both positive and negative directions [31]. In reality of course, at least at the macroscopic scale, plates are finite and the choice of boundary conditions potentially have a greater effect on the response of the system to load than if they are modelled as being completely remote from the location of the buckle pattern. Nevertheless, if situations arise for which the deflection is restricted to a small portion of the structure then we could say such buckle patterns are effectively localized in an engineering sense although not homoclinic according to a strict mathematical definition.

In order to make headway with our stated goal of introducing a second spatial dimension, it may seem natural to simply investigate the appropriate planar version of the SH equation; see for example [1, 23] for several investigations into 2D localized patterns possible with the planar SH. However, extending in a simple-minded manner hides the complication that a flat plate may respond in other ways when loaded. For instance, there is now the possibility of bending about two axes and twisting which gives the plate extra stiffness and hence offers a good solution for efficient design [29]. Furthermore, compatibility and the constitutive equations arising from the theory of elasticity need to be satisfied and this adds extra terms together with the need to introduce a new stress function which relates deformations and strains to stresses. For moderate to large deflections the bending of a flat plate is often modelled by the Föppl–von Kármán (FvK) equations for, although it is known that they have some limitations and inconsistencies, they have been shown to usefully model post-buckling plate behaviour at a qualitative level that is normally accurate enough for most engineering purposes [9].

We aim to study here the case where the behaviour of an elastic plate is modified owing to the presence of a supporting elastic foundation or substrate on which it rests. Depending on the detailed properties of the foundation different phenomena can be realized. We will discuss the various different buckling modes that are possible and how they relate to each other as the loading on the plate is varied. In order to demonstrate the potential usefulness of the plate model, we will mention a few examples from various fields that might

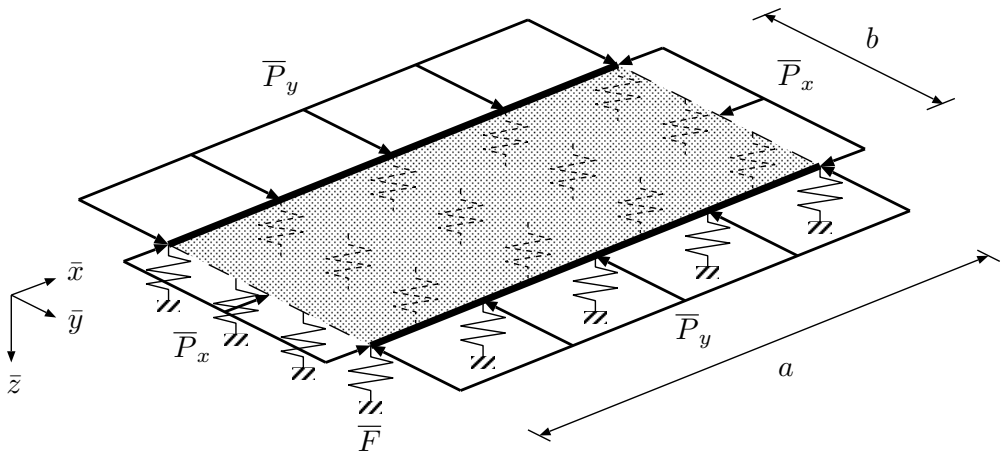

Figure 1: *Schematic representation of a thin rectangular plate supported on an elastic foundation. Fixed boundary conditions are applied on the long edges (denoted by the thick lines) while Neumann conditions are imposed on the shorter sides (dashed lines). The in-plane loading is $\bar{P}_x$ and $\bar{P}_y$ in the $\bar{x}$ and $\bar{y}$ directions respectively. The continuous foundation is represented as a series of elastic springs with resistance $\bar{F}$ given by (2.2)*

benefit from our findings.

An important feature of the plate model is that it necessarily involves separate loading parameters from two directions. For the one-dimensional strut any loading acts at a point and so cannot vary spatially but in two directions this constraint has to be relaxed; the loading in either direction need not be constant and, in general, would vary with position. Moreover proper consideration has to be taken of the aspect ratio of the plate. One might naïvely expect that a long thin plate might well respond to loading in a way similar to that of a strut but if the two dimensions of the plate are comparable then it is far from clear what one might expect to happen. It would not be surprising if in this case distinct phenomena occur that are peculiar to the strictly two-dimensional case.

The remainder of the paper is organized as follows. In §2, the model is formally introduced and in §3 a Galerkin method is used to obtain approximate buckling solutions which emerge from the flat fundamental state. These Galerkin predictions suggest how to conduct efficient full numerical solutions. A dynamical stability analysis described in §4 establishes criteria that predict when a one-dimensional (striped) solution may be unstable to transverse instability leading to a fully two-dimensional pattern. Fully numerical solutions are obtained and described in §5 and these are compared directly with the earlier results. The paper closes in §6 with some conclusions of the work and a look forward to possible further investigations of the problem.

2 Model formulation

The FvK equations for plates [29] have been shown to provide an accurate model for post-buckling behaviour and an analysis demonstrates that the naturally emerging post-buckling solutions are periodic in two orthogonal directions with the formation of a rectangular cellular pattern of undulations [13].

We consider a thin flat plate made of a homogeneous and isotropic material of Young's modulus E, Poisson's ratio ν and with thickness h as shown in Figure 1. The co-ordinate axes are aligned so that the mid-surface of the plate sits in the $\bar{x}$-$\bar{y}$ plane and the structure is supported in the $\bar{z}$-direction by an elastic foundation. Buckling is described by a system derived from the classical von Kármán equations [29] with the addition of terms accounting for the supporting elastic foundation together with an acceleration term based on the time $\bar{t}$ [2]. The incorporation of this acceleration will enable us to later examine the temporal stability of

solutions and then the key equations may be cast as

$$\rho h\bar{w}_{\bar{t}\bar{t}} + D\overline{\nabla}^4\bar{w} - h\left(\bar{\phi}_{\bar{y}\bar{y}}\bar{w}_{\bar{x}\bar{x}} + \bar{\phi}_{\bar{x}\bar{x}}\bar{w}_{\bar{y}\bar{y}} - 2\bar{\phi}_{\bar{x}\bar{y}}\bar{w}_{\bar{x}\bar{y}}\right) + \bar{P}_x\bar{w}_{\bar{x}\bar{x}} + \bar{P}_y\bar{w}_{\bar{y}\bar{y}} + \bar{F}(\bar{w}) = 0, \tag{2.1a}$$

$$\overline{\nabla}^4\bar{\phi} - E\left(\bar{w}_{\bar{x}\bar{y}}^2 - \bar{w}_{\bar{x}\bar{x}}\bar{w}_{\bar{y}\bar{y}}\right) = 0, \tag{2.1b}$$

in which $\overline{\nabla}^4$ denotes the biharmonic operator with respect to $\bar{x}$ and $\bar{y}$ and all subscripts on variables (but not parameters) denote partial differentiation with respect to the appropriate variable. Moreover $D = Eh^3/(12(1-\nu^2))$ denotes the bending stiffness of the plate, $\bar{w}(\bar{x},\bar{y},\bar{t})$ is its lateral displacement and $\bar{\phi}(\bar{x},\bar{y},\bar{t})$ the corresponding stress function. We note that the terms proportional to $\bar{P}_x$ and $\bar{P}_y$ account for the in-plane loading in the $\bar{x}$ and $\bar{y}$ directions respectively.

The crucial difference between our model and that for a plate supported only on its edges is the presence of the foundation resistance $\bar{F}(\bar{w})$ that acts across the plate. Here, following the methodology used for the corresponding strut problem, we take $\bar{F}$ to be of Winkler type [20] so that it is solely dependent on lateral deflection w and no shear interaction is present; then

$$\bar{F}(\bar{w}) = \bar{k}_1\bar{w} - \bar{k}_2\bar{w}^2 + \bar{k}_3\bar{w}^3, \tag{2.2}$$

where the $\bar{k}_j$ are constants and and whose values we discuss below.

Let us take the plate to be rectangular of dimensions $a \times b$ with the thickness $h \ll a, b$. Appropriate physical boundary conditions can then be of various types. The edges may be unsupported (free), simply-supported (that prevents deflection but allows rotation) or fully fixed. Each one of these conditions supplies two kinematic conditions on the deflection or its derivatives. We will study the case of clamped edges in the $\bar{y}$-direction and a periodic displacement along the $\bar{x}$-direction to simulate a thin layer bonded to the elastic foundation [38]. The cases we will study will consist of a plate with one of its centre lines on the $\bar{x}$-axis with length a and width b

$$\begin{aligned} \bar{w}(\bar{x},\pm b/2) = \bar{w}_{\bar{y}}(\bar{x},\pm b/2) = 0, \\ \bar{w}_{\bar{x}}(0,\bar{y}) = \bar{w}_{\bar{x}}(a,\bar{y}) = \bar{w}_{\bar{x}\bar{x}\bar{x}}(0,\bar{y}) = \bar{w}_{\bar{x}\bar{x}\bar{x}}(a,\bar{y}) = 0\,, \end{aligned} \tag{2.3}$$

with similar conditions imposed on $\bar{\phi}$. Note that the conditions along the $\bar{x}$-axis resemble the *symmetric-section* conditions used when seeking localized solutions to the one-dimensional strut model [20]. We will consider plates of various length in the $\bar{x}$ direction but, if periodic solutions are sought, then it suffices to use Neumann boundary conditions as above.

Let us pause here to consider the choice of the nonlinear foundation, $\bar{F}$, with a softening characteristic. Of course linearity is often an assumption made in order to simplify calculation or to deduce first-order behaviour. If we wish to delve deeper into phenomena then higher-order terms need to be considered and if we write out the response of the foundation as a Taylor series then it would seem natural next to incorporate a quadratic term. However, if we wish to explore a symmetric response with respect to vertical displacement then at least a cubic terms needs to be included as well. To decide the appropriate form of this term it should be remembered that in civil engineering contexts the foundation medium is frequently some form of soil. Most soils are a complex mixture of mineral particles and varying degrees of water content packed together in an irregular manner with many voids present. The interaction of solid granular particles, water and air is difficult to model but bulk properties can be derived and are often represented as a linear plus a softening leading-order nonlinear term with a negative coefficient. Where other structural systems such as sandwich panels have been modelled using a strut- or plate-on-foundation model similar softening nonlinearities have been introduced into the foundation to good effect [17, 19]. The rationale behind such an approximation is given in terms of the bulk behaviour of the central core material which is often a foam and its voids initially undergo collape when loading but then may subsequently restabilize due to contact of the solid walls of the material. The restabilization is modelled by a higher degree polynomial term with a positive coefficient.

In material manufacture, the response of an elastic substrate supporting the material has a complicated interaction relationship. To first order, it is often modelled as linear but as deformations develop, nonlinear responses are often observed [38] and can have significant effect on the overall behaviour of the material. In both of the above scenarios, the softening is only the initial deviation from nonlinearity for there is often some recovery of stiffness (restabilization) when higher-order kinematic effects are taken into account. We model this as the next order (cubic) term having a positive sign.

2.1 Non-dimensionalization

In order to analyse the system, it is helpful to scale variables to remove as many coefficients as possible. Therefore we set

$$\bar{x} = \lambda x, \quad \bar{y} = \lambda y, \quad \bar{w} = \mu_1 w, \quad \bar{\phi} = \mu_2 \phi, \quad \bar{t} = \xi t \tag{2.4}$$

where

$$\begin{aligned} &\lambda = \sqrt[4]{\frac{D}{\bar{k}_1}}, \quad \mu_1 = \sqrt{\frac{D}{Eh}}, \quad \mu_2 = \frac{D}{h}, \quad \xi = \sqrt{\frac{\rho h}{\bar{k}_1}}, \\ &P_x = \frac{\bar{P}_x}{\sqrt{\bar{k}_1 D}}, \quad P_y = \frac{\bar{P}_y}{\sqrt{\bar{k}_1 D}}, \quad k_2 = \frac{\bar{k}_2}{\bar{k}_1}\sqrt{\frac{D}{Eh}}, \quad k_3 = \frac{\bar{k}_3 D}{\bar{k}_1 Eh}. \end{aligned} \tag{2.5}$$

This leads to

$$w_{tt} + \nabla^4 w - (\phi_{yy} w_{xx} + \phi_{xx} w_{yy} - 2\phi_{xy} w_{xy}) + P_x w_{xx} + P_y w_{yy} + F(w) = 0\,, \tag{2.6}$$

$$\nabla^4 \phi - \left(w_{xy}^2 - w_{xx} w_{yy}\right) = 0, \tag{2.7}$$

where ∇^4 is the biharmonic operator with respect to the scaled variables x and y and $F(w) = w - k_2 w^2 + k_3 w^3$. In this scaled state, we suppose that the plate has length L and width γ.

2.1.1 Loading parameters and some simplifications

In the general nonlinear plate problem the loading parameters in the x and y directions, P_x and P_y, should be treated as independent. There is no necessity for either to be constant in space and such variation is likely to be of interest in provoking other behaviours such as bending about a lateral axis. We defer this extra degree of freedom as a refinement to be dealt with in a future study and instead concentrate solely on the case where both P_x and P_y are constant. That said, we will allow the possibility of either load being compressive (positive) or tensile (negative). It is conceptually easy to envisage different loading in the two directions: the simplest of course being uniaxial compression. Furthermore if the edges are prevented from moving in the plane by a pin or clamped support then tensile stresses can be built up as the plate deforms in the z direction as moderate to large buckling deformation increases. As outlined in Yang *et al.* [36], one-dimensional wrinkles can be induced in nanomaterials by pre-stretching the substrate and then depositing the material of interest on it. When the tensile force is released this results in a compression acting in one direction. Forces can then be applied in an orthogonal direction to induce further changes to the material.

In this study we will limit investigation to the case when, say, P_y is held constant and P_x is parametrically varied. Physically this is equivalent to preloading the plate in one direction (not necessarily up to the buckling capacity in that direction) and then applying another load in the orthogonal direction.

2.2 Total potential energy and Euler–Lagrange equations

We shall use the energy of the system as a measure of the various buckled states. The total potential energy associated with the non-dimensional form of the von Kármán equations in a slightly compacted form is [13]

$$\begin{aligned} V(w,\phi) =& \frac{1}{2}\int\int \left[(\nabla^2 w)^2 - 2(1-\nu)\left(w_{xx}w_{yy} - w_{xy}^2\right)\right] \mathrm{d}x\,\mathrm{d}y \\ &+ \frac{1}{2}\int\int \left[-(\nabla^2 \phi)^2 - 2(1+\nu)\left(\phi_{xx}\phi_{yy} - \phi_{xy}^2\right)\right] \mathrm{d}x\,\mathrm{d}y \\ &- \int\int \phi\left[-w_{xy}^2 + w_{xx}w_{yy}\right] \mathrm{d}x\,\mathrm{d}y \\ &- \frac{1}{2}\int\int \left[P_x w_x^2 + P_y w_y^2\right] \mathrm{d}x\,\mathrm{d}y \\ &+ \int\int \left[\frac{1}{2}w^2 - \frac{1}{3}k_2 w^3 + \frac{1}{4}k_3 w^4\right] \mathrm{d}x\,\mathrm{d}y. \end{aligned} \tag{2.8}$$

The first three lines of integrals represents the energy stored in the bending of the plate and includes nonlinear contributions arising from moderate to large deformations. The fourth line denotes the work done by the two loading parameters P_x and P_y and we identify the end-shortening of the plate in the x and y directions to be

$$\Delta_x = \frac{1}{2}\int\int w_x^2 \,\mathrm{d}x\,\mathrm{d}y \quad \text{and} \quad \Delta_y = \frac{1}{2}\int\int w_y^2 \,\mathrm{d}x\,\mathrm{d}y, \tag{2.9}$$

respectively. The final line of integrals in (2.8) gives the energy stored in the elastic foundation.

Of course, the governing equations are obtainable from V by obtaining the associated Euler–Lagrange equations of the system but the energy itself plays an important role in the preferential formation of certain buckle patterns.

2.3 Linearization

To understand the critical behaviour of the system it is necessary to linearize (2.6)-(2.7) about the trivial state. We will first look at the critical instability of an infinite plate so that boundary conditions can be safely ignored. In order to simplify the subsequent notation let us put $P_x = P$ and $P_y = \alpha P$ for where the parameter α can theoretically be any real value. However, without loss of generality, if we consider a plate that is longer in the x-direction than in the y then buckling will be dictated by P_x and so we can legitimately restrict our interest to $|\alpha| \leq 1$. If we then seek Fourier mode solutions

$$w(x,y) = A\mathrm{e}^{\Lambda x}\mathrm{e}^{\mathrm{i}\pi y}, \tag{2.10}$$

of the linearization of (2.6)-(2.7) about the trivial state, this gives

$$(\Lambda - \pi)^2(\Lambda + \pi)^2 + (\Lambda^2 - \alpha\pi^2)P + 1 = 0, \tag{2.11}$$

with solutions

$$\Lambda = \pm\frac{\sqrt{\pm\sqrt{S} - P + 2\pi^2}}{\sqrt{2}} \qquad S \equiv P^2 - 4\pi^2 P(1-\alpha) - 4. \tag{2.12}$$

A bifurcation occurs when S becomes negative and this then corresponds to x-spatially periodic modes. When $P < P^{\mathrm{C}}$ the eigenvalues are complex-valued with the critical values $P^{\mathrm{C}} = 2$ when $\alpha = 1$ and $P^{\mathrm{C}} = 2\pi^2 + \sqrt{\pi^4 + 1}$ when $\alpha = 0$; in contrast when $P > P^{\mathrm{C}}$ two of the eigenvalues are complex but the other two real. Of course we should also linearize equation (2.7) but as the result is independent of P it has no bearing on the bifurcation behaviour of the system with respect to load.

3 A Galerkin analysis

To obtain numerical solutions and then investigate their evolution under varying parameters it is necessary to derive an initial approximate two-dimensional solution to the system. Once a successful solution is obtained, we can employ numerical continuation to change P_y to the desired value.

We utilize a straightforward Galerkin procedure [33] for this purpose and start with a purely periodic response of the form

$$w = A\psi(x, y) \tag{3.1}$$

where A is a constant amplitude and ψ is an appropriate shape function. The initial stress function, ϕ, can be approximated either as a multiple of w or as zero if we are seeking to start from close to the bifurcation from the trivial state. We set the length of the plate in the x direction to be $L = \pi$ and impose Neumann boundary conditions in that direction. If the width $\gamma = 2$, then for clamped boundary conditions in the y-direction, at $y = \pm 1$, we need to identify an appropriate set of functions that satisfy $w(x, \pm 1) = w_y(x, \pm 1) = 0$. In the x-direction we assume Neumann boundary conditions, i.e., $w_x(0, y) = w_x(\pi, y) = 0$ and, furthermore, if $w(0, y) = w(\pi, y)$ then we have periodic boundaries in that direction. A suitable family of even functions obeying these boundary conditions is given by

$$\psi(x, y) = \cos mx((-1)^{n+1} + \cos n\pi y) \tag{3.2}$$

where m and n are integers which characterize the number of half waves occuring in the x and y directions, respectively and a periodic boundary condition in the x-direction requires m to be even. A counterpart odd set of functions in the y direction are given by

$$\psi(x, y) = \cos m\pi x \left(\sin n\pi y + \frac{n}{n+1} \sin(n+1)\pi y \right) \tag{3.3}$$

and in order to satisfy periodic boundary conditions in the x direction, m should be even. If we denote the left-hand side of the first equation (2.6) by $Q(x, y)$ and feed in the assumed form for w in (3.1) then the Galerkin formulation tells us that

$$\int_{y=-1}^{y=1} \int_{x=0}^{x=\pi} Q(x, y)\psi(x, y)\, \mathrm{d}x\, \mathrm{d}y = 0 \tag{3.4}$$

which leads to a cubic equation in A with a non-trivial even solution

$$A = \pm \frac{4}{\sqrt{105 k_3}} \sqrt{3m^2 P_x + \pi^2 n^2 P_y - (3m^4 + 2\pi^2 m^2 n^2 + \pi^4 n^4 + 3)}. \tag{3.5}$$

Note the presence of the cubic coefficient k_3 but the absence of the quadratic coefficient k_2. This feature is a consequence of taking a single term for the shape of w and leads to a symmetric from for A. For greater accuracy we could use more terms but since the motivation for this Galerkin method is simply to supply some initial functions that can be used to generate full numerical solutions close to the trivial one, there is little to be gained by deriving a more accurate initial state. For real values of A the term inside the square root must be greater than zero and this gives us a critical value for $P_x = P_x^C$, say, if P_y is held constant.

4 Transverse instability of quasi-1D states

We next examine the possibility of a transverse instability of quasi-1D states (by which we mean one-dimensional states that are trivially extended to two-spatial dimensions). We will subsequently find that the transverse instability of quasi-1D states play a pivotal role for the emergence of non-trivial 2D states.

We start by seeking solutions that vary only in the transverse direction y. If $W(y,t)$ is a one-dimensional solution of (2.6) and if $\Phi(y)$ satisfies (2.7) then it is immediately apparent that

$$W_{tt} + W_{yyyy} + P_y W_{yy} + f(W) = 0, \tag{4.1}$$

$$\mathrm{d}_y^4 \Phi = 0. \tag{4.2}$$

In such state, as there is no variation in x, the end-shortening component $\Delta_x = 0$ and the stress function $\Phi \equiv 0$ everywhere. It is well known that stationary solutions of (4.1), $W(y,t) = W(y)$, exist; see, for instance, see [24]. The linear stability properties of the stationary $W(y)$ with respect to perturbations in y can be inferred directly from results of the ubiquitous SH equation (given by (4.1) save that the W_{tt} is replaced by W_t). In particular, if a periodic orbit is linearly stable in the standard SH equation, then it is neutrally stable in (4.1). Hence, there do exist periodic orbits that are linearly stable with respect to perturbations in the y-direction.

We next consider a small transverse perturbation in the x-direction by letting $w(x,y,t) = W(y) + \hat{w}(x,y,t)$ and $\phi(x,y,t) = \hat{\phi}(x,y,t)$, where $\hat{w}$ and $\hat{\phi}$ are both small. Substituting these forms in (2.6) and (2.7) and linearizing we find

$$\hat{w}_{tt} + \nabla^4 \hat{w} - (\hat{\phi}_{xx}\, W_{yy}) + P_x \hat{w}_{xx} + P_y \hat{w}_{yy} + f'(W)\hat{w} = 0, \tag{4.3}$$

$$\nabla^4 \hat{\phi} + \hat{w}_{xx} W_{yy} = 0. \tag{4.4}$$

We look for periodic perturbations in the x-direction so that

$$\left\{\hat{w}, \hat{\phi}\right\} = \exp(\eta t + \mathrm{i}\beta x)\left\{\hat{v}(y), \hat{\psi}(y)\right\} + \text{c.c.}, \tag{4.5}$$

where c.c. denotes the complex conjugate, it follows that $\hat{v}$ satisfies the ODE eigenvalue problem

$$\eta^2 \hat{v} + \mathcal{L}_1(\hat{v}) + \beta^2 \hat{\psi} W_{yy} + \beta^4 \hat{v} - 2\beta^2 \hat{v}_{yy} - \beta^2 P_x \hat{v} = 0 \tag{4.6}$$

$$\mathcal{L}_2(\hat{\psi}) - 2\beta^2 \hat{\psi}_{yy} + \beta^4 \hat{\psi} - \beta^2 \hat{v} W_{yy} = 0 \tag{4.7}$$

in which the operators are

$$\mathcal{L}_1(\hat{v}) := \hat{v}_{yyyy} + P_y \hat{v}_{yy} + f'(W)\hat{v}, \quad \mathcal{L}_2(\hat{\psi}) := \hat{\psi}_{yyyy}. \tag{4.8}$$

We solve the spectral problem (4.6) for $\eta = \eta(\beta)$. For small β we write

$$(\eta, \hat{v}, \hat{\psi}) = (0, \hat{v}_0(y), 0) + \beta(\eta_1, \hat{v}_1(y), \hat{\psi}_1(y)) + \beta^2(\eta_2, \hat{v}_2(y), \hat{\psi}_2(y)) + \cdots \tag{4.9}$$

and at the zeroth and first orders it follows that $\hat{v}_0 = W_y$ and $\mathcal{L}_1(\hat{v}_1) = \mathcal{L}_2(\hat{\psi}_1) = 0$ so that $\hat{v}_1 \equiv 0$ and $\hat{\psi}_1 \equiv 0$.

At $\mathcal{O}(\beta^2)$, we have

$$\mathcal{L}_1(\hat{v}_2) = 2\hat{v}_{0,yy} + P_x \hat{v}_0 - \eta_1^2 \hat{v}_0, \qquad \mathcal{L}_2(\hat{\psi}_2) = \hat{v}_0\, W_{yy}. \tag{4.10}$$

A standard application of the method of adjoints leads to the conclusion that this system only admits an acceptable solution if

$$\eta_1^2 N_1^2 + 2N_2^2 - P_x N_1^2 = 0, \tag{4.11}$$

where $N_1 \equiv \int W_y^2 \,\mathrm{d}y$ and $N_2 \equiv \int W_{yy}^2 \,\mathrm{d}y$. Therefore the stability boundary is given by $\eta = \eta_1 \beta + \mathcal{O}(\beta^2)$ with

$$\operatorname{sgn} \eta_1^2 = \operatorname{sgn}(N_1^2 P_x - 2N_2^2). \tag{4.12}$$

This criterion for transverse instability replicates that for the standard SH equation [15]. In particular, it is known that 1D periodic orbits minimise their energy with respect to variation in their wavelength.

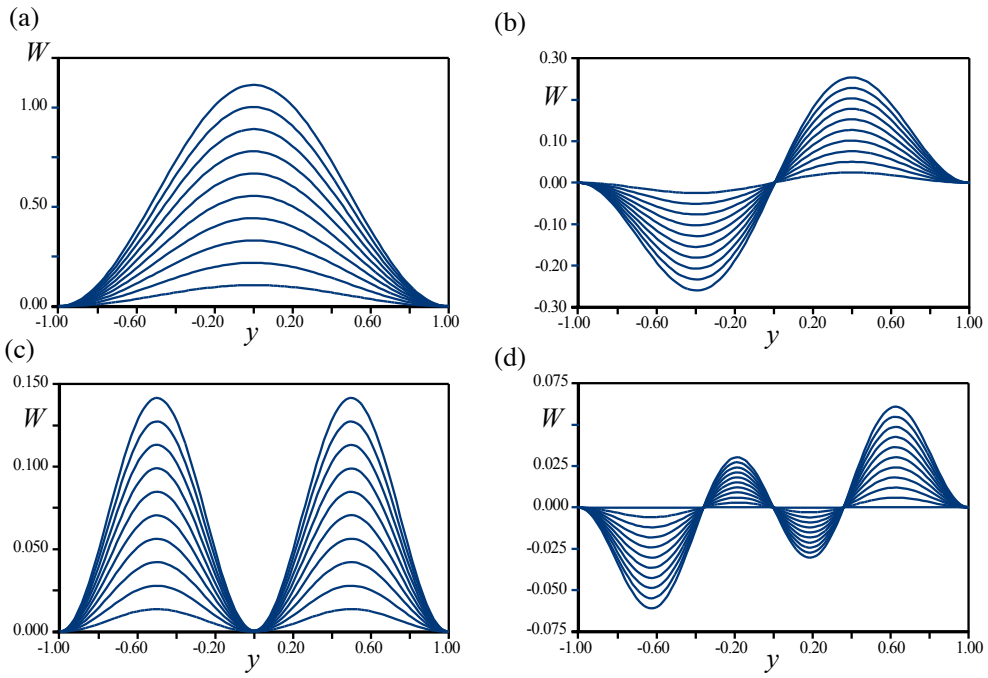

Figure 2: *Steady solutions of equation (4.1) with* $f(W) = W - 2W^2 + W^3/2$, *a normalized length* $L = 2$ *and various values of* P_y. *(a) first-mode,* $P^{\mathrm{C}} = 10.17$, *(b) second-mode,* $P^{\mathrm{C}} = 20.27$, *(c) third-mode,* $P^{\mathrm{C}} = 39.55$ *and (d) fourth-mode,* $P^{\mathrm{C}} = 59.71$.

We now have a procedure to predict the dynamical stability of patterns, at least when they start as functions of y alone. We therefore need to obtain solutions, $W(y)$, of the ODE (4.1), subject to appropriate boundary conditions (clamped in this case). Solutions can readily be obtained using AUTO [12] and the quantities N_1 and N_2 used to evaluate the transverse instability criterion (4.12). We compute the first four modes of (4.1) on a finite domain in y satisfying the boundary conditions (2.3) and the results are shown in Figure 2.

We show in Figure 3 a two-parameter plot of the transverse (in)stability region when $k_2 = 2$ and $k_3 = 0.5$. In this figure the values of N_1 and N_2 (see (4.11)) have been calculated numerically for a one-dimentional pattern and the boundary where the value of η_1^2 becomes positive (4.12) is shown. It indicates the value of P_x above which the solutions become unstable in time. We see that the location of the lower boundary for P_y is almost independent of P_x; indeed when $P_y \lessapprox 9.7$, the first-mode no longer exists and bifurcates from the flat state. We infer from this result that the striped (one-dimensional) solution remains stable until P_x is pushed beyond some ctitical value, after which it becomes unstable and the pattern evolves to some other state.

A word of caution is appropriate here. Our analysis described here is strictly only valid for a plate of infinite extent in the x-direction. Thus it is unlikely to provide a complete picture of the stability of plates of finite length for which the choice of boundary conditions ought to be relevant. That said, the analysis should provide some clue as to the types of behaviours that may be seen when a striped solution of a finite plate (with deflection independent of x) encounters a perturbation which varies in the transverse planar direction.

5 Numerical solutions

The above approximations allow us to speculate on the form of some of the possibilities of solution of the plate-on-foundation model. However, given the experience gained with related problems, such as the

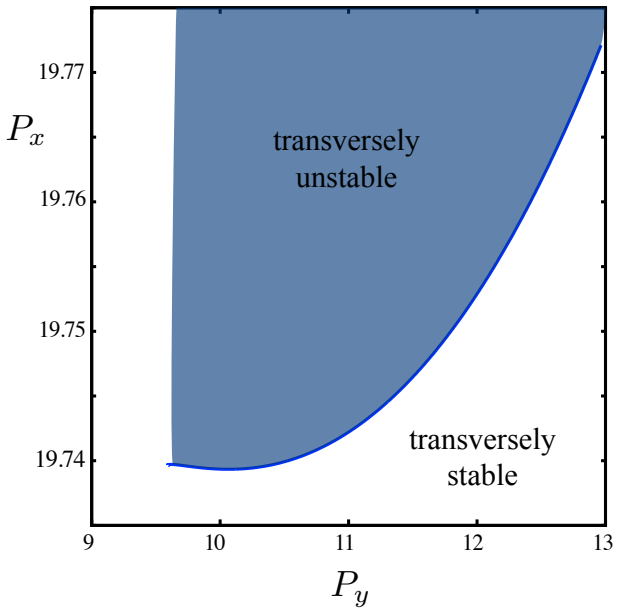

Figure 3: *Two-parameter plot of the transverse instability region for the first mode in Figure 2 for $k_2 = 2$ and $k_3 = 0.5$. The line shown marks the change in sign of η_1^2 (4.12) from negative (unshaded region) to positive (shaded region); the former are stable and the latter unstable. Note that the first mode cannot exist once $P_y \lessapprox 9.7$.*

(1D) strut model [32], it is highly probable that there is an intricate solution structure which, initially at least, can best be explored numerically. This was done by discretising the boundary value problem using a standard fourth order scheme in the x-direction and then imposing Neumann boundary conditions using ghost points [26]. A pseudo-spectral Chebyshev discretisation was employed in the y-direction with the clamped boundary conditions enforced by choosing the polynomial interpolant, $p(y)$, of a function in y to be $p(y) = (1 - y^2)q(y)$ where $q(y)$ is a polynomial with $q(\pm 1) = 0$; see Trefethen [30, Chapter 14]. The two-dimensional differentation operators were constructed using Kronecker products as described in [30] and the boundary value problem solved using a Newton trust region based algorithm [10]. We also embedded the boundary value problem into a secant continuation formulation to facilitate path following of the solutions in parameter space [21].

The scheme was implemented in MATLAB (version 2015a) with typical discretizations in x of $N_x = 41$ mesh points on $x \in [0, \pi]$ and $N_y = 21$ Chebyshev collocation points in y.

5.1 Periodic solutions

As mentioned earlier, it is frequently the case that for plate problems focus is concentrated on periodic behaviour particularly in the macroscopic example of engineering structures. In such instances the wavelength of the buckle pattern is of the same order of magnitude as the overall dimensions of the plates so only a relatively small number of waves are expected to span the whole domain. The aspect ratio is also important; a plate that is very much thinner in one dimension than the other might conceivably behave somewhat like a strut [34] but wider plates may well exhibit very different behaviour. We take some tentative numerical steps towards investigating this variation in §55.3.

The earlier Galerkin analysis suggested that solutions which are periodic both in x and y can bifurcate from the trivial flat state and they do so in pairs. However we now appreciate a limitation of the simple-minded Galerkin approximation used above because it is evident that, since the foundation is asymmetric with respect to deflection the pair of modes that evolve are not mirror images of each other. In order

to model this asymmetric behaviour, more than a single mode would be required to break the implicit symmetry [16]. Nevertheless, the single-mode approach gives us a firm connection between the one- and two-dimensional studies. A typical example of the periodic post-buckling regime is depicted in Figure 4. Here the two branches emerging from the flat state are labelled A and B and shown in different colours. In P-Δ_x space both branches overlap exactly and it is therefore more informative to present the plot with one extra dimension (here, deflection at the origin) to prise the two branches apart and show that they really are distinct. The buckled shape corresponds to $m = 3$, $n = 1$ as defined in (3.2). With $P_y = 2$, the prediction from the 1D approach in §4 is that at bifurcation $P_x \approx 17.03$ (see (4.12)) while the numerical solution of the full equation reveals that the bifurcation occurs at around $P_x = 22.7$. Each point on the curve is a solution of the static equilibrium equations although the energy V does vary considerably. The value of the energy can be loosely thought of as an informal relative measure of how distorted the deflected surface is, starting at zero at the bifurcation point (Bif) and dropping off as the striped solution is approached (St) (although as the striped solution is obviously not flat, the value of the energy is not zero).

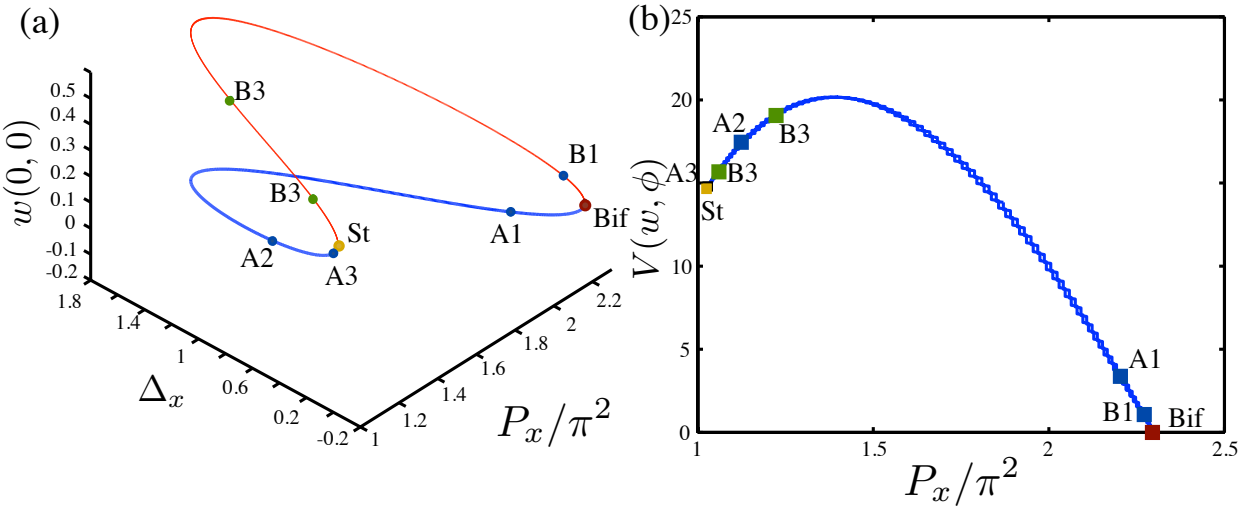

Figure 4: *(a) Bifurcation diagram and (b) potential energy plot of periodic solutions of the von Kármán plate-on-foundation model under in-plane forces with $k_2 = 2$ and $k_3 = 0.5$. The plate has length $L = \pi$ and the transverse load, P_y, is held constant at 2. The two branches are denoted A in blue (thick line), and B in red (thin line). (b) In P_x-V space the two branches are congruent and solutions corresponding to individual points identified on each branch are shown in Figures 5 and 6.*

Some solutions at various values of P_x are shown in Figures 5 and 6. In Figure 5(a) we see the buckle pattern, which emerges from the flat state $w = 0$. Of course, this solution relates to just one side of the bifurcation point as a second pattern, which is not quite the mirror image of the first, evolves on the other branch. Figures 5(b) and (c) depict solutions further into the post-buckling regime and it is much easier to see that these solutions are asymmetric about the flat state owing to the bias in the foundation introduced by the quadratic term.

Solutions on each branch continue to maintain the same structure as P_x is varied except that the amplitudes of both the peaks and troughs increase steadily until the branches near the striped solution St which is shown in Figure 6. This last state corresponds to the situation when the two branches eventually coalesce thus forming a closed bifurcation curve (isola) on which the solution appears to be trapped.

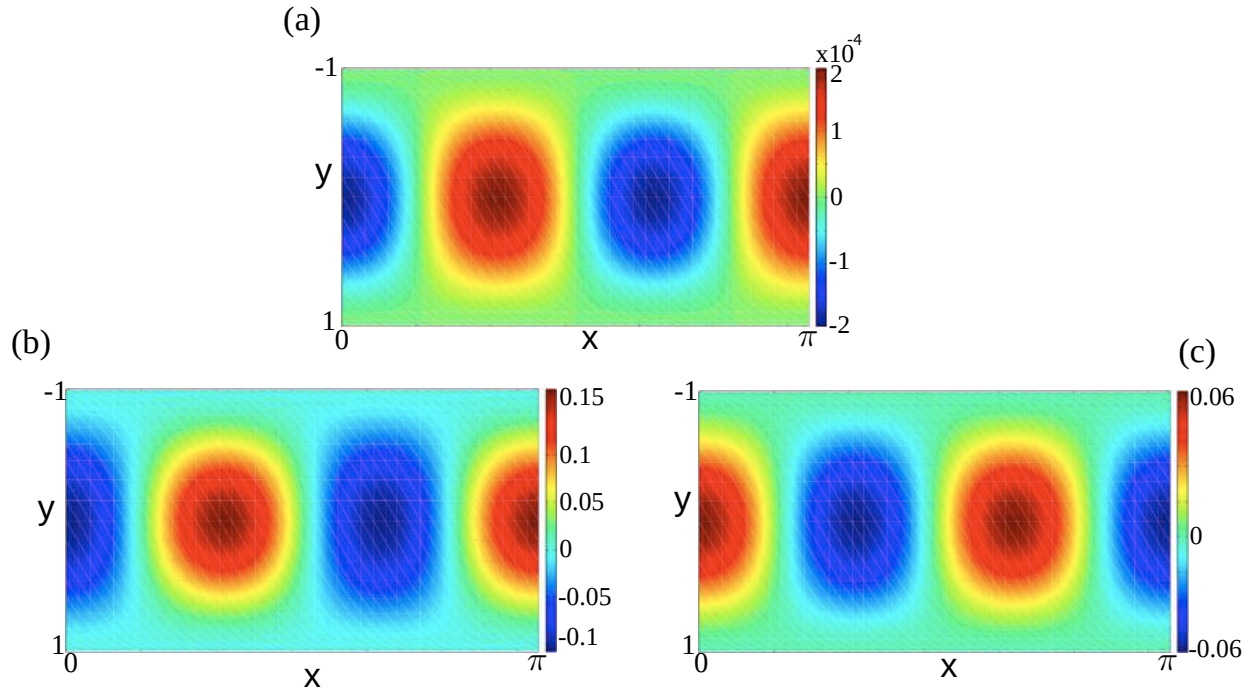

Figure 5: *Contours of $w(x, y)$ predicted by numerical solution of the von Kármán plate-on-foundation equations under in-plane forces. Domain of plate is $x \in [0, \pi]$ and $y \in [-1, 1]$. (a) Solution close to bifurcation point, denoted as Bif in Figure 4, $P_x = 22.695$. The indicated deformation, w, is in the range $\pm 2 \times 10^{-4}$. (b) Solution corresponding to Point A_1 in Figure 4, $P_x = 21.761$, $w \in [-0.11, 0.17]$. (c) Solution corresponding to Point B_1 in Figure 4, $P_x = 22.434$, $w \in [-0.085, 0.082]$. These solutions correspond to the even case with $m = 3$, $n = 1$ in §3.*

5.1.1 Striped solution

It is evident that a special example of a periodic solution is that discussed in §4 where the deflection is purely a function of y. The solution has been shown to be stable to a two-dimensional perturbation only if the axial load P_x lies within a certain range. Our computations above indicate that the solution represents a transition from solutions of one parity to another. The numerical results also confirm that Δ_x is zero both at the bifurcation from the trivial state *and* at the striped state (see Figure 4(a)). A very important distinction between these two limiting configurations is that the potential energy is quite different— see Figure 4(b). The upshot is that the two states are not interchangeable and a straightforward transition from one to the other is impossible.

For the same value of P_y (= 2), two further families of solutions can be found that both bifurcate from the fundamental state but which do so at different values of P_x (see Figures 7). The emerging solutions are distinct, having a different number of waves in the y direction but, as these solutions evolve, they converge to the same striped solution presented earlier. Though kinematically similar, it should be remembered that P_x is different in the two instances although the final striped solution has potential energy $V \approx 14.649$ (equation (2.8)). The potential energy of the striped solution is lower than other equilibrium states in the vicinity which satisfies the axiom for static stability [28] and numerically agrees with our analysis of dynamical stability in §4 that such solutions should be statically stable.

Two further bifurcation diagrams are presented for a different value of transverse load: $P_y = 7$ (see Figure 8). It can be seen once more that although the solutions emergent from the trivial state have separate forms, they again coalesce onto the same striped solution. In this case, $V \approx 73.821$.

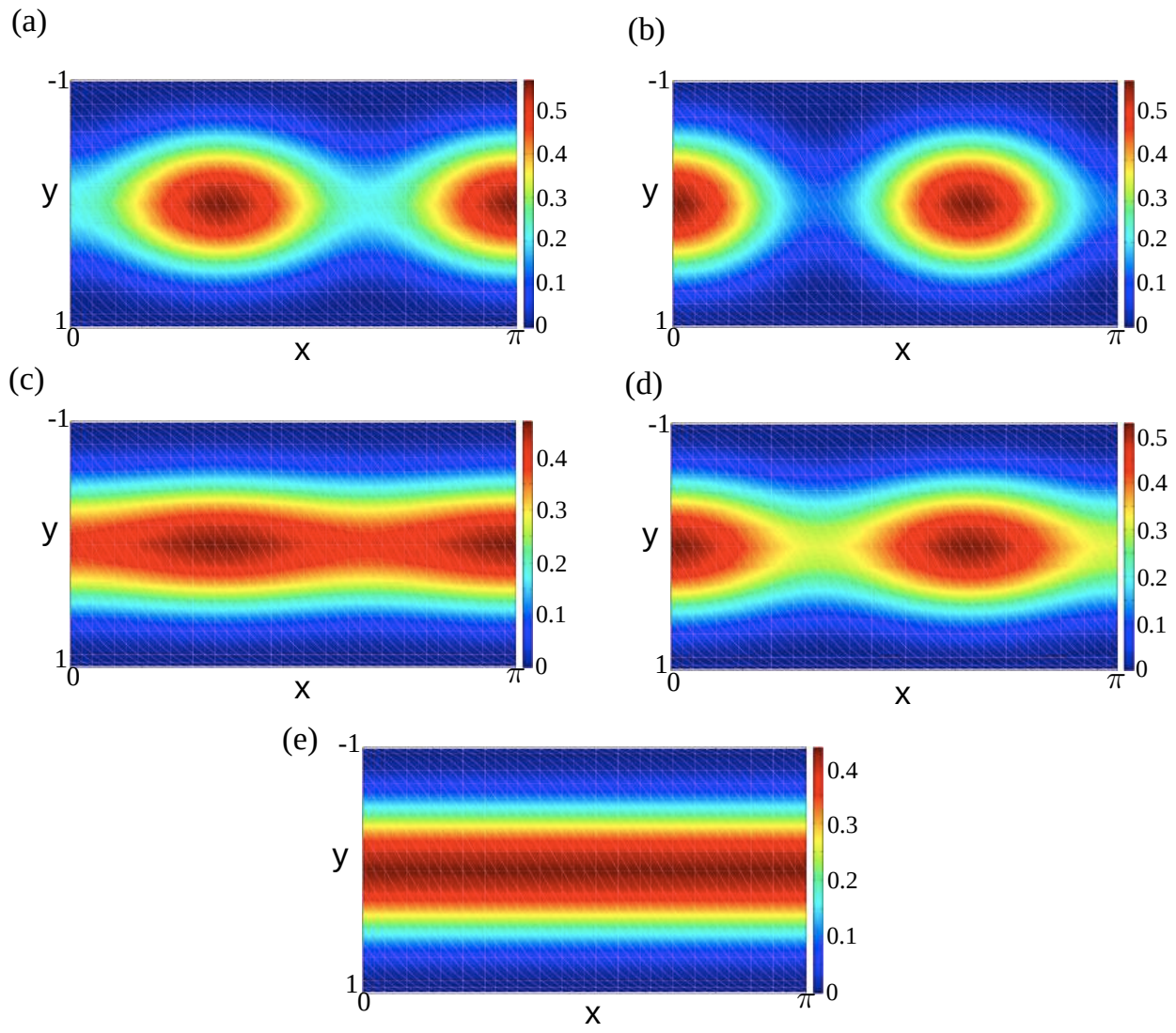

Figure 6: *Contours of $w(x, y)$ from numerical solutions using the equations and geometry of Figure 5. The five plots correspond to (a) Point A_2 in Figure 4 with $P_x = 11.126$ and $w \in [0, 0.57]$. Equivalent data for the remaining four plots are (b) B_2, $P_x = 12.070$ and $w \in [-0.01, 0.58]$; (c) A_3, $P_x = 10.153$ and $w \in [0, 0.47]$; (d) B_3, $P_x = 10.465$ and $w \in [0, 0.55]$; (e) limit point St, $P_x = 10.110$ and $w \in [0, 0.43]$.*

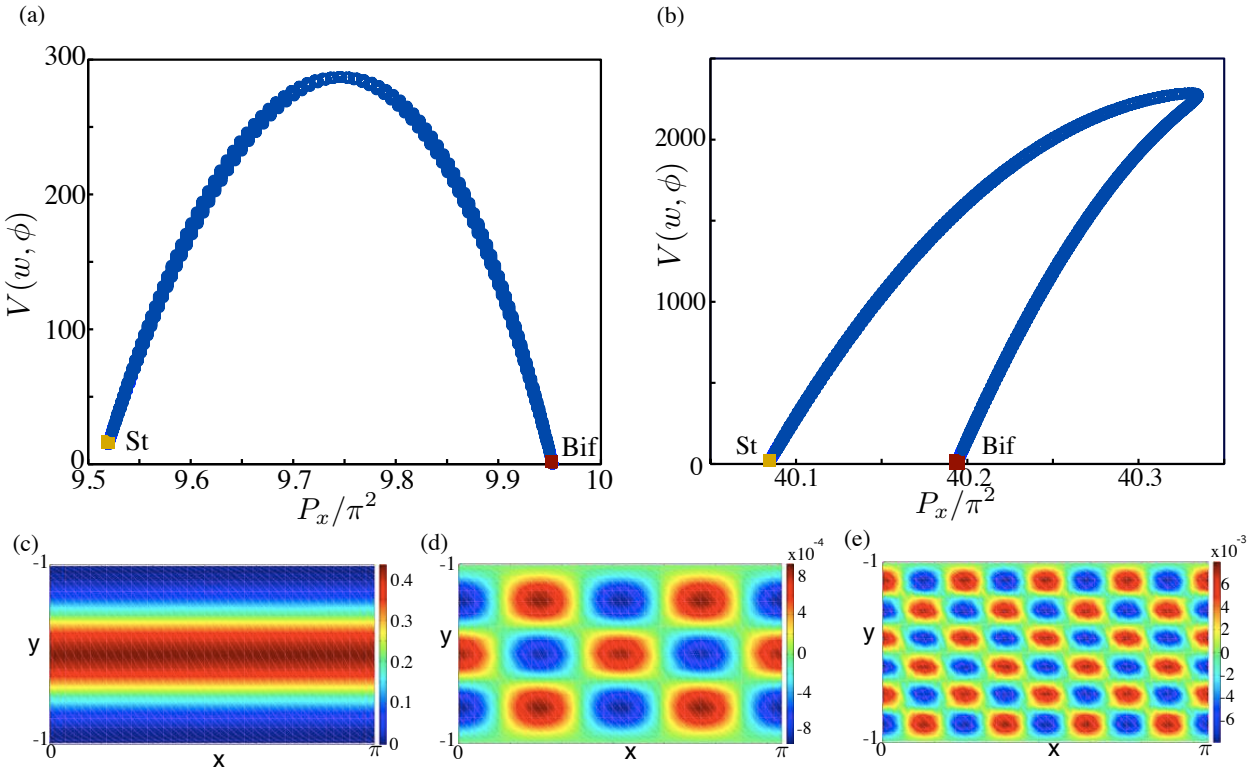

Figure 7: *Bifurcation diagrams of two periodic solutions of the von Kármán plate model under in-plane forces with* $k_2 = 2$ *and* $k_3 = 0.5$ *(a) even solution with* $m = 4$, $n = 2$ *and (b) odd solution with* $m = 8$, $n = 3$ *(see §3). The transverse load is* $P_y = 2$. *(c) Numerical solution at coalescent limit points St for both (a) and (b), with* $w \in [0, 0.43]$. *(d) Numerical solution of deformed plate near bifurcation point Bif in (a) with* $w \in [-9\times10^{-4}, 9\times10^{-4}]$. *(e) Numerical solution near bifurcation point Bif in (b) with* $w \in [-8\times10^{-3}, 8\times10^{-3}]$.

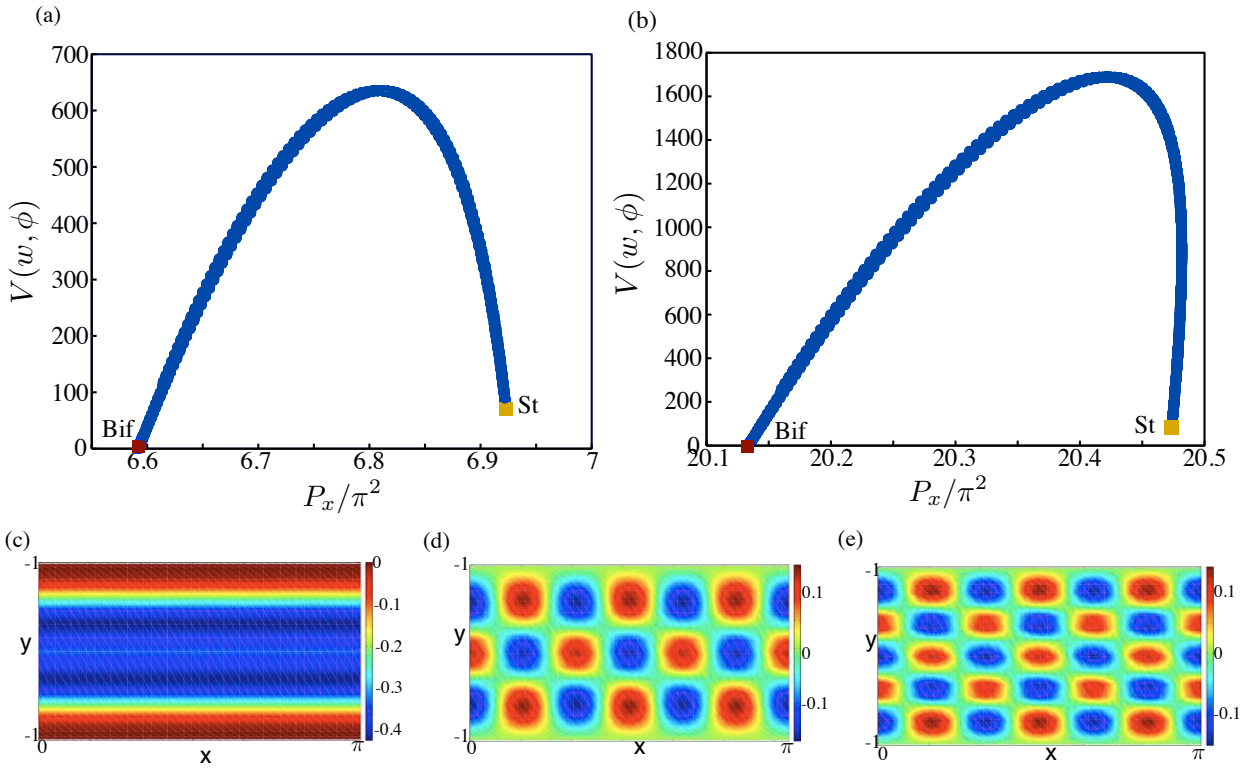

Figure 8: *Two bifurcation diagrams of periodic solutions of the von Kármán plate model under in-plane forces with* $k_2 = 2$ *and* $k_3 = 0.5$. *(a) An even solution with* $m = 6$, $n = 2$ *as defined in §3. (b) An even solution with* $m = 6$, $n = 3$. *In both cases, the transverse load,* P_y, *is held constant at 7. (c) Solution at coalescent limit points shown for both (a) and (b) as St with* $w \in [-0.42, 0]$. *(d) Numerical solution near bifurcation point Bif in (a) (*$w \in [-0.17, 0.2]$*). (e) Numerical solution near bifurcation point Bif in (b) (*$w \in [-0.2, 0.2]$*).*

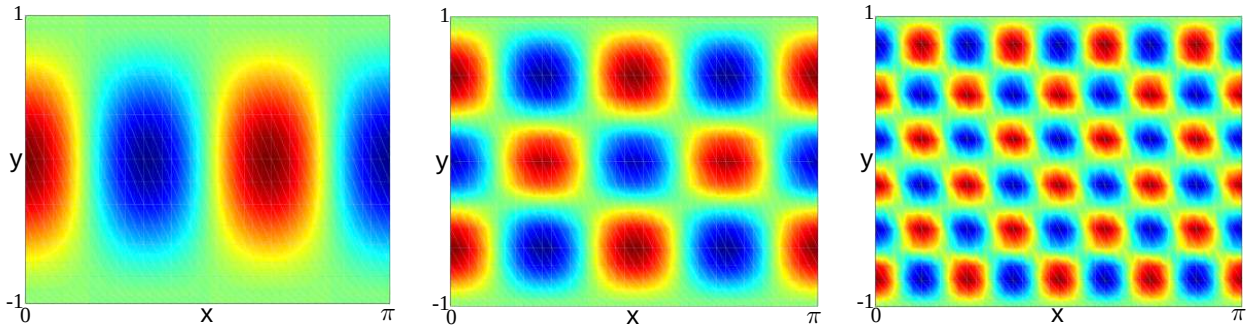

(a) $P_x/\pi^2 = 1.03$ (b) $P_x/\pi^2 = 9.52$ (c) $P_x/\pi^2 = 40.11$

Figure 9: *Eigenmodes of the striped solution depicted in Figure 6(e) for various critical values of P_x (with $P_y = 2$) for the cases (a) $P_x = 10.17$, (b) $P_x = 93.96$ and (c) $P_x = 395.9$. Plots shown in the domain $x \in [0, \pi]$ and $y \in [-1, 1]$.*

5.1.2 Transverse stability of the striped solutions

It is evident that the same striped solution exists at the limit point of several solutions bifurcating from the flat state (e.g. Figures 6(e) and 7(c) where three distinct two-dimensional bifurcating patterns share the same striped pattern or Figure 8(c) for two others for a different value of P_y). The form of these sets of one-dimensional solutions are dictated solely by the value of the load parameter P_y only because the end shortening in the x direction, Δ_x, is zero and so there is no contribution to the potential energy from P_x. On the other hand the form of the solutions emerging from the trivial state is dependent on both P_x and P_y. So, the question that inevitably arises is: how can the same striped solution be linked to multiple two-dimensionally periodic forms? The answer is guided both by the approximate analysis carried out in §4 and the numerical simulations.

Theoretical analysis reveals that the striped solution remains dynamically stable as long as

$$P_x < \frac{2N_2^2}{N_1^2}. \tag{5.1}$$

If P_x is larger than this limit then η_1 (4.12) is real and the solution will grow exponentially in time. The striped solution under consideration closely resembles mode 1 in Figure 2 and it is determined that the critical value of $P_x \approx 19.7$. This compares reasonably well with the numerically computed limit values of N_1 and N_2 for the full equations which lead to the prediction $P_x \approx 22.7$.

By numerically finding the striped solution for various value of P_x, bifurcations can be detected by numerically estimating when an eigenvalue of the approximate solution becomes zero. The structure of the eigensolution closely resembles the deflection pattern in the vicinity of critical buckling and a bifurcation is detected at around $P_x = 10.17$. The unstable eigensolution at this load is plotted in Figure 9(a) and it can be seen that although the actual deflected shape is one dimensional, the eigensolution reveals the direction in which any disturbance would grow. Thus we conclude that in the vicinity of this load, the solution would naturally evolve towards a pattern indicated by that unstable solution. Further transverse instabilities can be detected at various values of P_x (while holding P_y constant) and some are shown in Figure 9 (b) and (c). These unstable eigensolutions resemble the buckle patterns in Figures 7. The numerically determined values of P_x correlate very well with the values at the limit points of the bifurcation curves. Thus we conclude that the same striped pattern can indeed be linked to various two-dimensional patterns in a systematic way.

We have found that for each given P_y, there is an associated striped solution. However, we can subsequently induce buckle patterns of different types by then loading the plate in the orthogonal direction, P_x. Theoretically, this could be used as a way of producing desired deflection pattern in a repeatable manner. A consequence of the phenomenon of multiple patterns being able to develop from a particular 1D striped

mode could be used to manufacture a layer of material with a desired pattern in a two-step process. Firstly, the specimen could be loaded in one in-plane direction to give a striped buckle shape and then judicious loading in the orthogonal direction would then give rise to the required 2D pattern. In particular, carefully varying the secondary load would, in principle, be a possible method of manufacturing materials with various tuneable patterns and hence physical properties [36].

5.2 Localized behaviour

As we indicated in the previous section, periodicity is the predominant form of behaviour to be expected in most plated structures since the finite domain precludes genuinely localized solutions which are only evident over an infinite domain. However, if the domain is significantly larger than the natural wavelength of the buckle pattern then a (periodic) solution can arise which comes to resemble its truly localized counterpart in the sense that over the whole extent of the plate, only a small fraction undergoes noticeable deflection. Localization of patterns can be favourable under certain conditions, particularly where a softening nonlinearity makes such a pattern energetically more favourable to jump to than its periodic counterpart [16] even though both are kinematically admissible. Even in the case that such localized solutions are unstable, they can form critical (mountain pass) modes [14] to other forms. Thus a localized solution may develop in a structure of finite extent if at one end the solution and all its derivatives approach zero. Such is the case for the buckling of a thin cylindrical shell [18]. In other applications, such as contemporary material science, periodic buckling has been the primary focus [37]. However, if the extent of the domain is much larger than the wavelength of buckle patterns then isolated (localized) patterns can coexist with periodic solutions.

To demonstrate the relationship between periodic and localized forms, Figure 10 shows the bifurcation structure of two plates of non-dimensional lengths 10 and 20. These plots can be interpreted as a localized patterns with symmetry about the postion $x = 0$. As can be seen, a pair of solutions bifurcate from the trivial (zero-energy) state, the other is a subsidiary solution forming a multi-humped pattern [32]. We infer that as length increases the limiting behaviour will be localized states that bifurcate from the unbuckled state and co-exist with their periodic counterparts just as in the one-dimensional strut model [16]. For a finite-length plate, the way in which a localized pattern may be realized is by an initial periodic pattern which is then disturbed, perhaps by a secondary bifurcation, into a localized state. Such multi-staged buckling phenomena are common in plates [17, 19].

5.3 Aspect ratio

The problem as formulated in this study consists of an investigation into the theoretical buckling aspects of a structure that extends into two dimensions. The equivalent one-dimensional problem (the strut model) has been extensively studied but the plate on a foundation has attracted far less interest. There are many potential avenues to explore for this model and we have hinted at some possible ideas here. In many ways, it is perhaps the role played by the aspect ratio that is perhaps most fundamental so we introduce the aspect ratio, $l_y \equiv \gamma/L$, as a continuous parameter. In Figure 11 we illustrate the evolution of a basic periodic solution as l_y is varied from its original value $l_0 = 2/\pi$. As the ratio is increased so the pattern spreads to fill the extra width and yet the buckled cells approximately maintain their own aspect ratio. As the width gets larger, there are a few transitions when the number of cells increases by one each time; this is clearly a form of mode jumping [13]. Further evidence that lends credence to this conclusion is provided in the plot of potential energy versus l_y as the curve exhibits undulations at the point where the number of buckle cells changes.

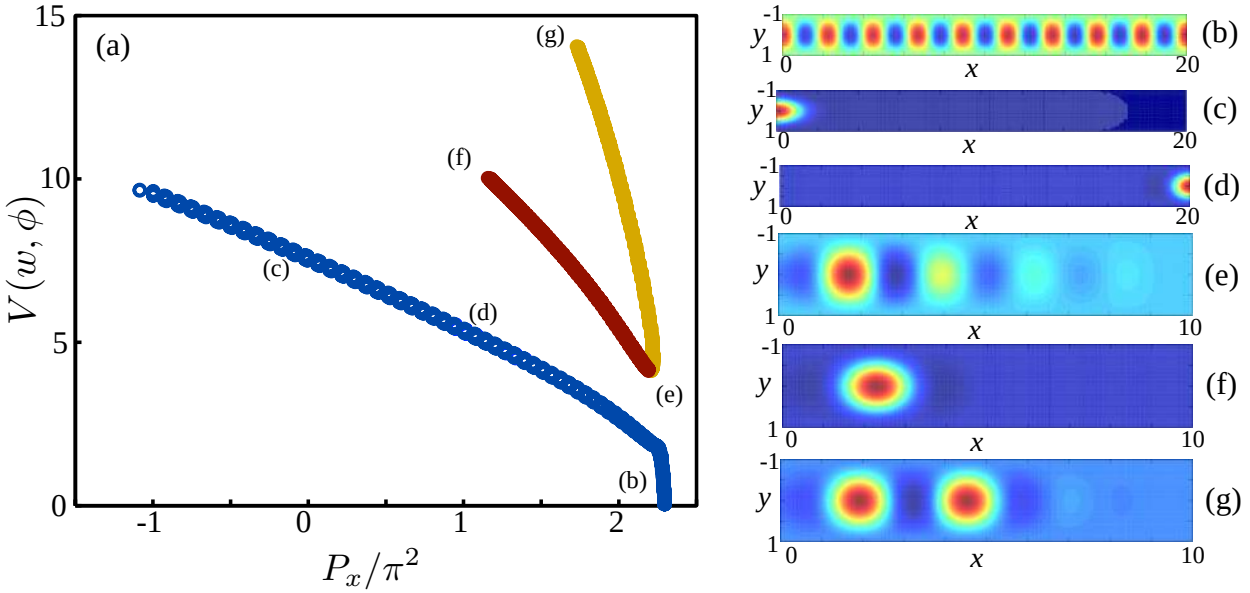

Figure 10: *Localized solutions of the plate. Two families are shown in the bifurcation diagram (a): a primary solution calculated over* $x \in [0, 20]$ *(blue) bifurcating from the trivial state with deflections shown in (b) near the bifurcation point itself* ($w \in [-7 \times 10^{-3}, 7.1 \times 10^{3}]$*); (c) and (d) further down the two branches (seen as a single line as the overlap)* ($w \in [0, 0.62]$*; and a secondary solution calculated over* $x \in [0, 10]$ *with deflections shown at the limit point (e)* ($w \in [-0.11, 0.24]$*) at the end of each of the branches (f) and (g) (shown as red (dark) and yellow (light) respectively) and* $w \in [-0.03, 0.53]$ *and* $w \in [-0.12, 0.42]$*, respectively.*

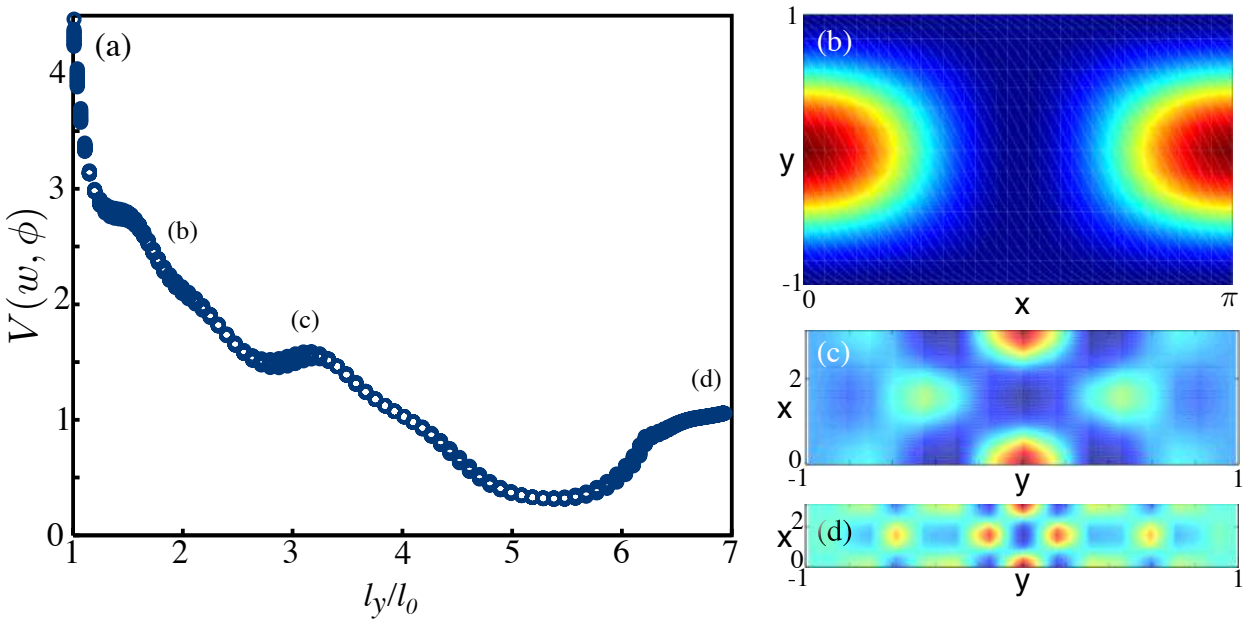

Figure 11: *Aspect ratio variation for* $P_x = 19.74$*,* $P_y = 2$*,* $k_2 = 2$ *and* $k_3 = 0.5$*. (a) Variation of total potential energy,* V *against aspect ratio. (b) Solution with original aspect ratio* $l_0 = 2/\pi$ *(*$w \in [-0.10, 0.32]$*). (c) Continued solution with* $l_y = 3.2468 l_0$ *(*$w \in [-0.05, 0.14]$*) and (d) solution with* $l_y = 6.9393 l_0$ *(*$w \in [-0.04, 0.06]$*). Note that plots (c) and (d) have been rotated through* 90°*.*

6 Conclusions and further study

The current work has examined the fundamental behaviour of a structural system in order to investigate the effect of adding an extra spatial dimension to a well-studied one-dimensional problem. As expected, the introduction of a finite width opens up a new richness of possibilities of solutions available after buckling ensues. The loading regime is seen to be enhanced with the ability to apply different forces in different directions and indeed to allow the loading to vary spatially, although that has been left for future work.

We have seen that some conventional techniques, such as the Galerkin method, are able approximately to capture buckling behaviour emergent from the flat state but fully numerical methods are needed to follow what happens to these solutions further into post-buckling. We found that there are special one-dimensional (striped) patterns which eventually connect both the branches which emerge from the critical state and furthermore that the same striped pattern (governed by the transverse load, P_y) can lie at the end of multiple branches. The unstable eigensolutions of the striped solution reveal which two-dimensional (spot) solution it links to. An interesting possibility arises from our findings in that we have outlined a plausible procedure by which material could be manufactured with pre-determined characteristics by careful application of load in one in-plane direction followed by loading at right angles to it. This technique could be a simpler alternative to current methods used to manufacture highly-tuned nanomaterials.

A straightforward analysis of the striped solution using an adaptation of the strut model [34] reveals information about the stability of solutions and this, coupled to numerics, has enabled us to locate the boundary between stable and unstable behaviour. The boundary gives a reasonable approximation for the longitudinal load at which the striped solution gives way to spots or cellular buckle patterns.

Although we have considered the loading as two independent parameters this study, it may be instructive in future to allow the load to vary along either or both edges in order to simulate various conditions that may arise in reality. An example of such varying stress may arise through thermal expansion or contraction of a plate embedded in an elastic medium. Some consideration has been given to localized behaviour and the effects of aspect ratio. These features would increase in importance were we to look at the case where the buckling cells are small compared with the length and width of the plate.

The plate–foundation model has been used to mimic many physical situations ranging from material wrinkling in industrial manufacturing [11], theoretical neo-Hookian materials [5] and fold hierarchies in thin films [25] through to the morphological development of tissue and organs such as the brain [4]. However, most modelling usually starts with some simplifying assumptions including the reduction of the problem into one-dimensional phenomena. We offer here a way to begin systematically to study two-dimensional behaviour which holds the possibility of uncovering a much richer set of competing and interacting solutions. Although resolution is presently far off, progress in this direction may conceivably go some way to explain some of the complex behaviour observed in practice.

Ethics: This work did not involve any experiments on living organisms.

Data Accessibility: Calculations were performed using equations which are all published in this paper and numerical computations were carried out using published algorithms with MATLAB.

Funding: The research was funded as part of the authors' standard employment contracts.

Authors' Contributions: MKW conceived of the problem, MKW and DJBL designed the programme of study and MKW undertook the Galerkin calculations and computations based on numerical algorithms developed by DJBL. MKW and APB worked on the reduced one-dimensional stability problem and DJBL devised a numerical verification method for these results. All authors contributed to the writing of the paper and approved its final submission.

Competing Interests: The authors had no competing interests in performing this work.

Acknowledgements: We express our thanks to Professor Geoffrey Nash at the University of Exeter for

helpful discussions regarding the manufacture and properties of modern two-dimensional materials and undergraduate David Frampton, also at the University of Exeter, for helping to develop the MATLAB code to find the Galerkin approximations in §3. Finally, we are grateful to the referees for their helpful comments which considerably enhanced the presentation of this work.

References

[1] D. Avitabile, D. J. B. Lloyd, J. Burke, E. Knobloch, and B. Sandstede, *To snake or not to snake in the planar Swift–Hohenberg equation*, SIAM J. Appl. Dyn. Syst., 9 (2010), pp. 704–733.

[2] N. Baddour and J. W. Zu, *A revisit of spinning disk models. Part I: Derivation of equations of motion*, Appl. Math. Model., 25 (2001), pp. 541–559.

[3] F. Brau, H. Vandeparre, A. Sabbah, C. Poulard, A. Boudaoud, and P. Damman, *Multiple-length-scale elastic instability mimics parametric resonance of nonlinear osciallators*, Nature Physics, 7 (2011), pp. 56–60.

[4] S. Budday, P. Steinman, and E. Kuhl, *Secondary instabilities modulate cortical complexity in the mammalian brain*, Philos. Mag., 95 (2015), pp. 3244–3256.

[5] Y. P. Cao and J. W. Hutchinson, *From wrinkles to creases in elastomers: the instability and imperfection-sensitivity of wrinkling*, Proc. R. Soc. Lond., 468 (2011), pp. 94–115.

[6] A. Castellano-Gomez, M. Poot, G. A. Steele, H. S. J. van der Zant, N. Agraït, and G. Rubio-Bollinger, *Elastic properties of freely suspended MoS_2 nanosheets*, Adv. Mater., 24 (2012), pp. 772–775.

[7] A. R. Champneys, G. W. Hunt, and J. M. T. Thompson, *Localization and solitary waves in solid mechanics*, Philos. Trans. Roy. Soc. London Ser. A, 355 (1997), pp. 2077–2081.

[8] S. J. Chapman and G. Kozyreff, *Exponential asymptotics of localised patterns and snaking bifurcation diagrams*, Physica D, 238 (2009), pp. 319–354.

[9] P. G. Ciarlet, *A justification of the von Kármán equations*, Arch. Rational Mech. Anal., 73 (1980), pp. 349–389.

[10] T. F. Coleman and Y. Li, *An interior trust region approach for nonlinear minimization subject to bounds*, SIAM J. Optim., 6 (1996), pp. 418–445.

[11] T. J. Dodwell, R. Butler, and G. W. Hunt, *Out-of-plane ply wrinkling defects during consolidation over an external radius*, Composites Science and Technology, 105 (2014), pp. 151–159.

[12] E. J. Doedel, B. E. Oldeman, A. R. Champneys, F. Dercole, T. F. Fairgrieve, Y. A. Kuznetsov, B. Sandstede, X. Wang, and C. Zhang, AUTO-07p*: Continuation and bifurcation software for ordinary differential equations.* Available from `http://indy.cs.concordia.ca/auto/`, 2009.

[13] P. R. Everall and G. W. Hunt, *Arnold tongue predictions of secondary buckling in flat plates*, J. Mech. Phys. Solids, 47 (1999), pp. 2187–2206.

[14] J. Hor/'ak, G. J. Lord, and M. A. Peletier, *Cylinder buckling: The mountain pass as an organizing center*, SIAM J. Appl. Math., 66 (2006), pp. 1793–1824.

[15] R. B. Hoyle, *Pattern formation*, Cambridge University Press, Cambridge, 2006.

[16] G. W. Hunt, H. M. Bolt, and J. M. T. Thompson, *Structural localization phenomena and the dynamical phase-space analogy*, Proc. R. Soc. Lond., A 425 (1989), pp. 245–267.

[17] G. W. Hunt and L. S. da Silva, *Interactive bending behavior of sandwich beams*, ASME J. Appl. Mech., 57 (1990), pp. 189–196.

[18] G. W. Hunt, G. J. Lord, and A. R. Champneys, *Homoclinic and heteroclinic orbits underlying the post-buckling of axially-compressed cylindrical shells*, Comput. Meth. Appl. Mech. Eng., 170 (1999), pp. 239–251.

[19] G. W. Hunt and M. A. Wadee, *Localization and mode interaction in sandwich structures*, Proc. R. Soc. Lond., A 454 (1998), pp. 1197–1216.

[20] G. W. Hunt and M. K. Wadee, *Comparative lagrangian formulations for localized buckling*, Proc. R. Soc. Lond., A 434 (1991), pp. 485–502. doi:10.1098/rspa.1991.0109.

[21] B. Krauskopf, H. M. Osinga, and J. Galan-Vioque, eds., *Numerical Continuation Methods for Dynamical Systems*, Springer, 2007.

[22] C. Lee, X. Wei, J. W. Kysar, and J. Hone, *Measurement of the elastic properties and intrinsic strength of monolayer graphene*, Science, 321 (2008), pp. 385–388. doi:10.1126/science.1157996.

[23] D. J. B. Lloyd, B. Sandstede, D. Avitabile, and A. R. Champneys, *Localized hexagon patterns of the planar Swift–Hohenberg equation*, SIAM J. Appl. Dynam. Syst., 7 (2008), pp. 1049–1100.

[24] L. A. Peletier and W. C. Troy, *Spatial patterns*, Progress in Nonlinear Differential Equations and their Applications, 45, Birkhäuser Boston, Inc., Boston, MA, 2001.

[25] P. M. Reis, *Folded in hierarchy*, Nature Mater., 10 (2011), pp. 907–909.

[26] G. D. Smith, *Numerical Solution of Partial Differential Equations Finite Difference Methods*, Oxford University Press, 2003.

[27] J. M. T. Thompson, *Advances in shell buckling: Theory and experiments*, Int. J. Bif. Chaos, 25(1530001) (2015).

[28] J. M. T. Thompson and G. W. Hunt, *A general theory of elastic stability*, Wiley, London, 1973.

[29] S. P. Timoshenko and S. Woinowsky-Krieger, *Theory of plates and shells*, McGraw-Hill, Singapore, 2nd ed., 1970.

[30] L. N. Trefethen, *Spectral methods in MATLAB*, vol. 10 of Software, Environments, and Tools, Society for Industrial and Applied Mathematics (SIAM), Philadelphia, PA, 2000.

[31] L. N. Virgin, *Vibration of axially loaded structures*, Cambridge University Press, 2007.

[32] M. K. Wadee and A. P. Bassom, *Effects of exponentially small terms in the perturbation approach to localized buckling*, Proc. R. Soc. Lond., A 455 (1999), pp. 2351–2370. doi:10.1098/rspa.1999.0407.

[33] M. K. Wadee, Y. Higuchi, and G. W. Hunt, *Galerkin approximations to static and dynamic localization problems*, Int. J. Solids Struct., 37 (2000), pp. 3015–3029.

[34] M. K. Wadee, G. W. Hunt, and A. I. M. Whiting, *Asymptotic and Rayleigh–Ritz routes to localized buckling solutions in an elastic instability problem*, Proc. R. Soc. Lond., A 453 (1997), pp. 2085–2107. doi:10.1098/rspa.1997.0112.

[35] N. Xu, B. L. Wang, H. Q. Sun, and F. J. Kong, *Rippling and the external electric field on conductance in corrugated graphene nanoribbons molecular device*, Physica B, 406 (2011), pp. 756–759.

[36] S. X. Yang, C. Wang, H. Sahin, H. Chen, Y. Li, S.-S. Li, A. Suslu, F. M. Peeters, Q. Liu, J. B. Li, and S. Tongay, *Tuning the optical, magnetic, and electrical properties of $ReSe_2$ by nanoscale strain engineering*, Nano Lett., 15 (2015), pp. 1660–1666. doi:10.1021/nl504276u.

[37] C. Zhang, J. Song, and Q. Yang, *Periodic buckling patterns of graphene/hexagonal boron nitride heterostructure*, Nanotechnology, 25 (2014).

[38] Y. Zhao, Y. Cao, W. Hong, M. K. Wadee, and X.-Q. Feng, *Towards a quantitative understanding of period-doubling wrinkling patterns occurring in hyperelastic bilayer systems*, Proc. R. Soc. Lond., A 471 (2015). Art. no.: 20140695.